Journal of Applied Physics ARTICLE scitation.org/journal/jap

Participation of nitrogen impurities in the growth of grown-in oxide precipitates in nitrogen-doped Czochralski silicon

Cite as: J. Appl. Phys. **131**, 155703 (2022); doi: 10.1063/5.0082542
Submitted: 16 December 2021 · Accepted: 25 March 2022 ·
Published Online: 19 April 2022

Tong Zhao, Defan Wu, Wu Lan, Deren Yang, and Xiangyang Ma[a)]

AFFILIATIONS

State Key Laboratory of Silicon Materials and School of Materials Science and Engineering, Zhejiang University, Hangzhou 310027, China

[a)]**Author to whom correspondence should be addressed:** mxyoung@zju.edu.cn

ABSTRACT

For nitrogen-doped Czochralski (NCZ) silicon, it is well known that nitrogen (N) and oxygen (O) impurities can interact to form nitrogen–oxygen shallow thermal donors (N–O STDs); moreover, the N impurities can be involved into heterogeneous nucleation to facilitate the formation of grown-in oxide precipitates. However, how the N impurities participate in the growth of grown-in oxide precipitates during the post-anneal remains unclear. Besides, the correlation between the formation of N–O STDs and the growth of grown-in oxide precipitates is yet to be revealed. In this work, the effects of pre-anneals at temperatures of 900–1200 °C on the formation of N–O STDs at 650 °C in NCZ silicon have been first investigated. Thus, it has been found that the more significant growth of grown-in oxide precipitates during the pre-anneal, which consumes much more N impurities, leads to forming much fewer N–O STDs. This finding stimulates us to explore the mechanism for the participation of N impurities in the growth of grown-in oxide precipitates. To this end, the capture of N impurities by the oxide precipitates, on the one hand, and the release of N impurities from the oxide precipitates, on the other hand, have been investigated by two systematically constructed experiments. The obtained results enable us to reasonably propose that the N impurities participating in the growth of grown-in oxide precipitates predominately reside at the oxide precipitate/Si interfaces, which reduces the interfacial energies, thus favoring the growth of grown-in oxide precipitates. Such a viewpoint is well supported by the density functional theory calculations. In a word, this work has gained an insight into the mechanism for the participation of N impurities in the growth of grown-in oxide precipitates, starting from exploring the correlation between the formation of N–O STDs and the growth of grown-in oxide precipitates.

I. INTRODUCTION

The interaction between nitrogen (N) and oxygen (O) impurities in Czochralski (CZ) silicon has long been a subject matter of interest. It is indicated that certain N–O complexes formed at 300–650 °C are characteristics of single-electron shallow donors, with ionization activation energies of 34–37 meV.[1–13] Thus, such N–O complexes are termed as N–O shallow thermal donors (N–O STDs). Voronkov *et al.* found that the saturated concentration of the N–O STDs, formed at 600–650 °C, depends on the N concentration approximately by a square-root law.[14] Considering that the nitrogen pair (N_2) featuring a di-interstitial is the primary form of N impurities in silicon at low temperatures (e.g., 650 °C and below),[15–17] they deduced that a single N–O STD contains only one N atom, which is in accord with the result of the theoretical study conducted by Jones and co-workers.[18] Alt *et al.* and Wagner *et al.* experimentally proved that the N–O STDs are composed of one O atom, two or three O atoms through the investigations on the relationship between the concentration of N–O STDs and that of interstitial O (O_i) atoms in N-doped CZ (NCZ) silicon.[19,20] The previous studies have proved that the N–O STDs can be eliminated at temperatures 900 °C and above.[10,21] Moreover, our recent work indicates that the elimination of N–O STDs depends strongly on the annealing temperature ranging from 900 to 1200 °C. Thus, we have explored the mechanism for the elimination of N–O STDs.[22] As a matter of course, how the pre-anneals at 900–1200 °C affect the formation of N–O STDs, which is the inverse proposition of our recent work as mentioned above, is worthy to be answered.

Because the internal gettering associated with oxygen precipitation (OP) is critical for increasing the manufacturing yields of integrated circuits, the effects of N-doping on OP in CZ silicon have been investigated everlastingly in the past few decades.[23–26] It is known that the N impurities are involved in the heterogeneous nucleation in a manner to facilitate the formation of grown-in oxide precipitates.[27–34] Thus, the grown-in oxide precipitates in the NCZ silicon are with both higher density and larger sizes than those in the conventional CZ silicon.[29,30,34] By comparison, how the N impurities affect the growth of grown-in oxide precipitates has been less investigated. Nakai *et al.* reported that more grown-in oxide precipitates could grow up in NCZ silicon because the N-doping increased the number of grow-in oxide precipitates, which could be stable at higher temperatures with respect to those in the conventional CZ silicon.[29] However, they did not clarify how the N impurities behaved during the growth of grown-in oxide precipitates. Evidently, such remaining puzzle needs to be addressed.

As mentioned above, both the formation of N–O STDs and the growth of grown-in oxide precipitates involve the N impurities. Then, the correlation between such two processes is worthy to be revealed. In this work, we have first investigated how the pre-anneals at 900–1200 °C affect the formation of N–O STDs at 650 °C. It is found that the formation of N–O STDs, which is associated with the decrease in the concentration of (N_2)s, differs significantly due to the different pre-anneals that simultaneously result in the growth of grown-in oxide precipitates. Such results stimulate us to explore the mechanism for the participation of N impurities in the growth of grown-in oxide precipitates, which is manifested by the loss of (N_2)s. To this end, we have designed experiments from two aspects. On the one hand, a few of CZ silicon slices are subjected to the specific anneals to form different amounts of oxide precipitates, followed by the rapid thermal anneal (RTA) terminated at 1250 °C for 60 s in nitrogen (N_2) ambient for introducing N impurities. Through investigating the total N concentration and the concentration of (N_2)s in each CZ silicon slice as mentioned above, the capture of N impurities by the oxide precipitates can be learned. On the other hand, a few of NCZ silicon slices are first annealed at 1000 °C for 8 h, leading to the substantial growth of grown-in oxide precipitates and to the annihilation of (N_2)s. Subsequently, they are subjected to the RTA terminated at 1250 °C for different dwelling times. Through investigating the increases in the concentrations of (N_2)s and O_i atoms in the aforementioned NCZ silicon slices along with the dwelling time at 1250 °C, the correlation between the regeneration of (N_2)s and the dissolution of oxide precipitates can be revealed. Based on the results of the two experiments mentioned above, it is believed that the N impurities diffuse in the form of interstitial N (N_i) atoms toward the grown-in oxide precipitates growing up at the elevated temperatures (e.g., 900–1200 °C). Ultimately, the involved N impurities are predominantly located at the interfaces between the oxide precipitates and the silicon host (denoted as SiO_x/Si interfaces, $1 < x < 2$), which reduces the interfacial energies of oxide precipitates, thus facilitating the growth of grown-in oxide precipitates. In order to verify the above viewpoint, a supercell containing the α-SiO_2/Si interface is constructed. Then, the energy of the supercell, where an N atom is placed into the Si host, at the α-SiO_2/Si interface or into α-SiO_2, is calculated by density functional theory (DFT). As a result, it is indicated that the energy of the supercell where the N atom is located at the α-SiO_2/Si interface is lowest. Such a theoretical calculation result strongly supports the aforementioned viewpoint derived from the experimental study. In a word, this work has revealed the mechanism for the participation of N impurities in the growth of grown-in oxide precipitates, starting from investigating the effects of pre-anneals at 900–1200 °C on the formation of N–O STDs at 650 °C.

II. EXPERIMENTAL DETAILS

Two 150 mm-diameter, phosphorus (P)-doped n-type, ⟨100⟩-oriented CZ wafers were used. One was co-doped with N impurities (NCZ silicon wafer) and the other was free of N impurities (CZ silicon wafer). After the double-sided polishing, the two wafers were ∼1 mm thick. The concentrations of dopants and impurities in the two wafers are shown in Table I. Herein, the O_i concentrations ($[O_i]$s) were measured by room temperature (RT) Fourier transformation infrared (FTIR) spectroscopy using a calibration coefficient of 3.14×10^{17} cm^{-2}. The N concentration ([N]) was measured by secondary ion mass spectroscopy (SIMS). The P concentrations ([P]s) were transformed from the electrical resistivities measured by four-point probe (FPP) according to ASTM F723-88. The carbon concentrations in the two wafers were below the detection limit (5.0×10^{15} cm^{-3}) of FTIR spectroscopy. A number of specimens with a size of 1.5×1.5 cm^2 were cleaved from each wafer for different anneals and characterizations.

All the NCZ silicon specimens were first subjected to the pre-anneals at 900, 1000, or 1200 °C for 1–8 h, followed by the measurement of resistivities by FPP and by the detection of O_i atoms and (N_2)s by RT FTIR spectroscopy. The NCZ silicon specimen with the 2 h pre-anneal at 900, 1000, or 1200 °C was subsequently annealed at 650 °C for up to 8 h, during which the resistivity of the specimen was measured every 2 h by FPP at RT. Finally, all the 650 °C/8 h-annealed specimens were characterized by FTIR spectroscopy at 8 K. One NCZ silicon specimen with the 1000 °C/8 h pre-anneal was subsequently annealed at 1250 °C for 2 h, followed by the characterization of RT FTIR spectroscopy. Then, this specimen received 650 °C/8 h anneal to form N–O STDs, which were detected by FTIR spectroscopy at 8 K. Moreover, several NCZ silicon specimens with the 1000 °C/8 h pre-anneal were subjected to the RTA terminated at 1250 °C, which was ramped up from RT with a rate of 100 °C/s, for different dwelling times ranging from 0 to 30 s, followed by the cooling process at a rate of 50 °C/s. Such treated specimens were characterized by RT FTIR spectroscopy and were then etched in Schimmel etchant [HF (49%): CrO_3 (1 mol/l) = 1: 1 in volume ratio] for 15 min, followed by the observation of bulk microdefects (BMDs) related to OP by optical

TABLE I. The concentrations of dopants and impurities in the two silicon wafers used.

Silicon wafer	[P] (cm^{-3})	[O_i] (cm^{-3})	[N] (cm^{-3})
NCZ	2.50×10^{14}	8.00×10^{17}	2.06×10^{15}
CZ	1.50×10^{14}	8.10×10^{17}	…

microscopy (OM). All the aforementioned anneals were performed in argon (Ar) ambient. Moreover, after the anneal at 1000, 1200, or 1250 °C, each specimen was mechano-chemically polished to remove a layer of ~50 μm, which contained the out-diffusion zone of O and/or N impurities.

Three CZ silicon specimens were first subjected to the 1250 °C/2 h anneal for the substantial elimination of the grown-in oxide precipitates. Then, two of such specimens further received the two-step anneals of 800 °C/4 h + 1000 °C/4 h and 800 °C/4 h + 1000 °C/16 h, respectively, resulting in the decreases in $[O_i]$ ($\Delta[O_i]$s) of 1.47×10^{17} and 5.85×10^{17} cm^{-3}, derived from the measurements by RT FTIR spectroscopy. All the aforementioned anneals were performed in Ar ambient. The three specimens were mechano-chemically polished to remove a layer of ~50 μm, which contained the out-diffusion zone of O impurities. After the standard RCA cleaning and the terminal dip into the dilute HF solution [HF (49%): H_2O = 1:10 in volume ratio) for 30 s, the three specimens were subjected to the RTA terminated at 1250 °C, which was ramped up from RT with a rate of 100 °C/s, for a dwelling time of 60 s in N_2 ambient, followed by the cooling process at a rate of 50 °C/s. Such RTA in N_2 ambient was employed to introduce N impurities into the CZ silicon specimens involved. For the convenience of description, the three specimens that experienced the aforementioned annealing procedures are denoted as CZ-A, B, and C, respectively. Furthermore, Table II summarizes the annealing schemes for CZ-A, B, and C silicon specimens. It should be mentioned that most of the oxide precipitates, generated by the forgoing multiple anneals, in CZ-B and C silicon specimens were dissolved by the 1250 °C/60 s RTA in N_2 ambient, making $\Delta[O_i]$s to be decreased to 1.4×10^{16} and 8.6×10^{16} cm^{-3}, respectively. For the characterizations of CZ-A, B, and C silicon specimens, SIMS was employed to measure the depth profile of N concentration, RT FTIR spectroscopy was used to record the intensity of 963 cm^{-1} absorption peak related to the (N_2)s; OM was used to observe the BMDs delineated by 15 min etching in Schimmel etchant. Finally, CZ-A, B, and C silicon specimens received the 650 °C/8 h anneal, before and after which the resistivities were measured by FPP.

Lastly, it should be pointed out that the RT FTIR spectrum of each NCZ silicon specimen investigated in this work was obtained by subtracting that of the CZ control, whose $[O_i]$ and thickness were nearly the same as those of the NCZ silicon specimen. Moreover, the CZ control and the investigated NCZ silicon specimen received the same anneal.

TABLE II. The annealing schemes for three CZ silicon specimens investigated.

Specimen	Annealing scheme
CZ-A	1250 °C/2 h (in Ar ambient) + 1250 °C/60 s (in N_2 ambient)
CZ-B	1250 °C/2 h + 800 °C/4 h + 1000 °C/4 h (in Ar ambient) +1250 °C/60 s (in N_2 ambient)
CZ-C	1250 °C/2 h + 800 °C/4 h + 1000 °C/16 h (in Ar ambient) +1250 °C/60 s (in N_2 ambient)

III. THEORETICAL CALCULATIONS

The DFT calculations were run in the VASP code.[35–37] A supercell containing a SiO_2/Si interface was constructed for geometric optimization as the basic unit. Herein, the SiO_2/Si interface is composed of the (100) plane of silicon and that of α-SiO_2. Based on such a basic unit, other supercells where an N atom was placed into the silicon host, at the α-SiO_2/Si interface, and into α-SiO_2 were constructed, respectively. In the DFT calculations, the Perdew–Burke–Ernzerhof (PBE) exchange correlation functional at the General-Gradient-Approximation (GGA) level was adopted,[38–40] a $2 \times 2 \times 2\,k$ point sampling of the Brillouin zone and a plane wave basis set with a cutoff energy of 450 eV were employed. Moreover, the structure was optimized until the force on each atom was less than 0.01 eV/Å, and the threshold of calculations for energy comparison was 1.0×10^{-5} eV.

IV. RESULTS AND DISCUSSION

A. Effects of pre-anneals at 900–1200 °C on the formation of N–O STDs

Figure 1(a) shows the variation of carrier concentration in the NCZ silicon specimen along with the time of 650 °C anneal following the pre-anneal at 900, 1000, or 1200 °C for 2 h. It is well known that the oxygen-related thermal donors and the N–O STDs can be annihilated by the anneal for sufficient time (e.g., 2 h) at 900 °C and above.[10,22] Moreover, the generation of new donors at 650 °C requires several tens of hours.[41] Therefore, the increase in carrier concentration, as shown in Fig. 1(a), is resulted from the formation of fresh N–O STDs at 650 °C. As can be seen in Fig. 1(a), the carrier concentration in the specimen with the 1000 °C/2 h pre-anneal hardly changes with the annealing time at 650 °C, while that in the specimen with the 900 °C/2 h or the 1200 °C/2 h pre-anneal increases remarkably after 2 h anneal at 650 °C and then maintains nearly constant with the extension of 650 °C anneal. By comparison, the carrier concentration increases more significantly in the specimen with the 1200 °C/2 h pre-anneal.

Figure 1(b) shows the 8 K far-infrared FTIR spectra for those specimens of Fig. 1(a), with the subsequent 650 °C/8 h anneal. The absorption bands peaking at 240.4 cm^{-1} (N–O-3), 242.5 cm^{-1} (N–O-4), and 249.8 cm^{-1} (N–O-5), respectively, are well documented to correspond to the N–O STDs in different forms.[20,42] As can be derived from Fig. 1(b), the concentration of N–O STDs is highest in the specimen with the 1200 °C/2 h pre-anneal, while that is negligible in the specimen with the 1000 °C/2 h pre-anneal and that in the specimen with the 900 °C/2 h pre-anneal lies in between. Apparently, the result revealed by the FTIR spectra shown in Fig. 1(b) is consistent with that manifested by the variation of carrier concentration as shown in Fig. 1(a).

Figure 1(c) illustrates the middle-infrared FTIR spectra for the specimens subjected to the pre-anneals at 900, 1000, and 1200 °C for 2 h, respectively. For reference, the FTIR spectrum of the as-received specimen is also included in Fig. 1(c). It is well known that the N impurities in NCZ silicon exist predominantly in the form of (N_2)s at RT, corresponding to a pronounced IR absorption peak at 963 cm^{-1}.[15] It can be inferred from Fig. 1(c) that the

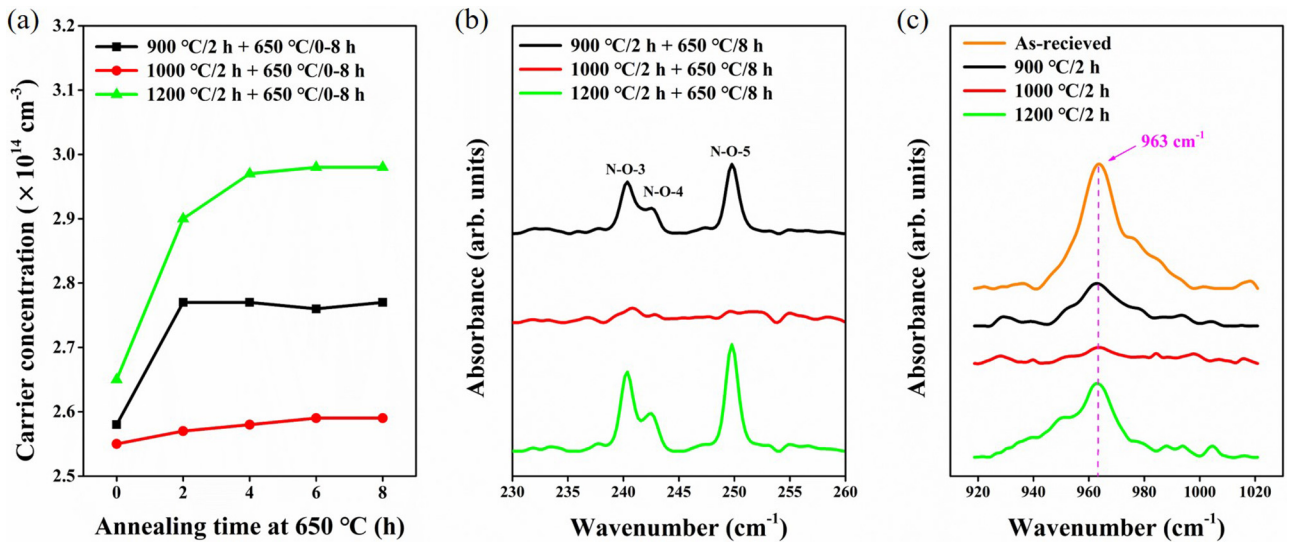

FIG. 1. (a) The variation of carrier concentration in the NCZ specimen along with the time of 650 °C anneal following the pre-anneal at 900, 1000, or 1200 °C for 2 h. (b) 8 K far-infrared FTIR spectra for those specimens of (a), annealed at 650 °C for 8 h. (c) RT middle-infrared FTIR spectra for the specimens subjected to the pre-anneals at 900, 1000, and 1200 °C for 2 h, respectively. The spectrum of the as-received specimen is included for reference.

concentration of (N_2)s in the as-received specimen is highest and that in the specimen with the 1200 °C/2 h pre-anneal is a little bit decreased comparatively. Moreover, the concentration of (N_2)s in the specimen with the 900 °C/2 h pre-anneal is further lowered and that in the specimen with the 1000 °C/2 h pre-anneal is negligible.

In brief, Fig. 1 shows that the concentrations of the remaining (N_2)s after the pre-anneals at 900–1200 °C for 2 h are quite different, leading to the different concentrations of N–O STDs formed by the subsequent 650 °C anneal, which is due to that the N atoms involved in the formation of N–O STD are decomposed from (N_2)s at 650 °C.[22,43]

B. The correlation between the growth of grown-in oxide precipitates and the formation of N–O STDs

Figure 2(a) shows the variation of $[O_i]$ in the NCZ silicon specimen along with the time of pre-anneal at 900, 1000, or 1200 °C. As seen, $\Delta[O_i]$ is significant due to the pre-anneal at 1000 °C, while that is slight in the case of pre-anneal at 1200 °C. Moreover, $\Delta[O_i]$ due to the pre-anneal at 900 °C lies in between. It should be mentioned that $\Delta[O_i]$ is resulted from the growth of grown-in oxide precipitates during the pre-anneal at 900, 1000, or 1200 °C. As is known to all, the higher the annealing temperature, the lower the supersaturation of O_i atoms (unfavorable for OP) while the faster the diffusion of O_i (favorable for OP). Therefore, it is understandable that the growth of grown-in oxide precipitates in the specimen with the pre-anneal at 1000 °C is the most significant, as shown in Fig. 2(a). Moreover, OP generally becomes more and more significant with the extension of anneal at a given temperature as long as the supersaturation of O_i atoms retains. $[O_i]$ of NCZ silicon used in this work is 8.0×10^{17} cm^{-3}, well above the solid solubility of O_i atoms (5.73×10^{17} cm^{-3}) in silicon at 1200 °C.[44] Besides, only a small part of grown-in oxide precipitates with relatively large sizes can grow up at 1200 °C. Hence, it still can be considered that the growth of grown-in oxide precipitates actually becomes increasingly significant with the extension of 1200 °C anneal, despite that $\Delta[O_i]$ manifested in Fig. 2(a) is not so noticeable.

Figure 2(b) shows the decrease in the intensity of the 963 cm^{-1} IR absorption peak associated with (N_2)s along with the time of pre-anneal at 900, 1000, or 1200 °C for each specimen of Fig. 2(a). It can be seen that the intensity of the 963 cm^{-1} peak decreases significantly with the extension of annealing time at each temperature. Remarkably, as the annealing time at 1000 °C is extended to 2 h and above, the intensity of the 963 cm^{-1} peak is negligible, meaning that (N_2)s have been substantially annihilated. This is also the case as the pre-anneal at 900 °C is prolonged to 8 h. While, in the case of pre-anneal at 1200 °C, the 963 cm^{-1} absorption peak is still discernible even as the annealing time reaches 8 h, indicating that a small amount of (N_2)s still remain in the specimen.

Figure 2(c) shows the concentrations of N–O STDs formed by the 650 °C/8 h anneal for the NCZ silicon specimens with the pre-anneals at 900, 1000, or 1200 °C for 1–8 h. Herein, the abscissa represents the time of pre-anneal. As can be seen, the concentration of N–O STDs decreases remarkably with the extension of pre-anneal at each temperature, keeping step with the decrease in the concentration of (N_2)s as revealed in Fig. 2(b).

In brief, Fig. 2 definitely indicates that (N_2)s become increasingly fewer and even are annihilated with the extension of pre-anneal at 900, 1000, or 1200 °C, during which the growth of grown-in oxide precipitates simultaneously proceeds. In other words, (N_2)s successively vanish into the grown-in oxide

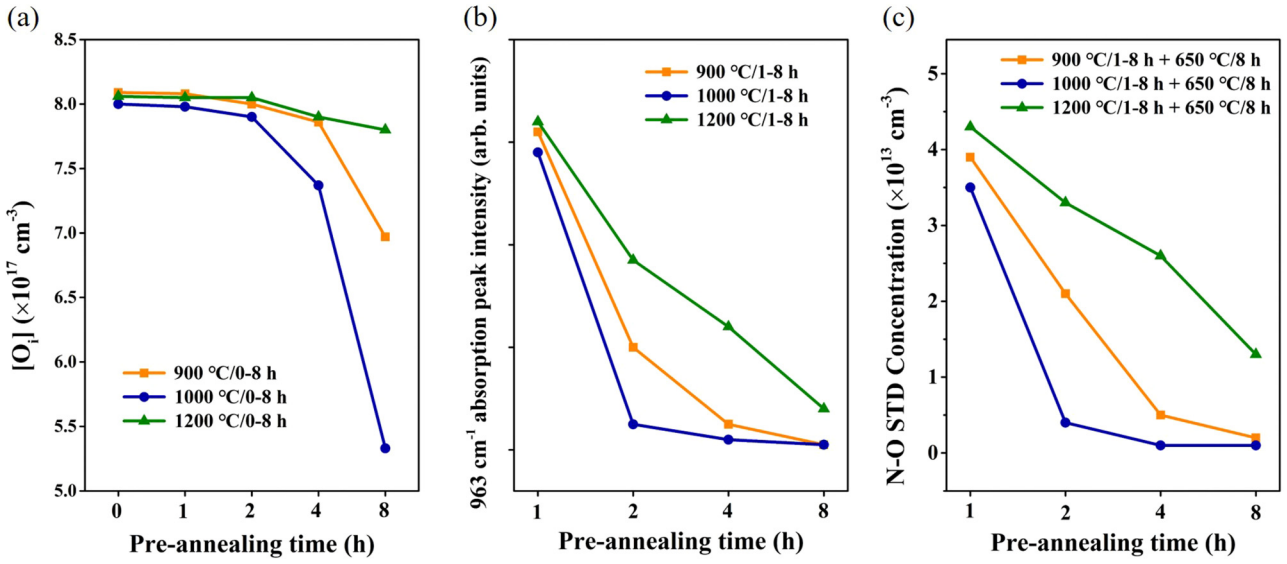

FIG. 2. (a) The variation of $[O_i]$ in the NCZ silicon specimen along with the time of pre-anneal at 900, 1000, or 1200 °C. (b) The decrease in the intensity of the 963 cm^{-1} IR absorption peak along with the time of pre-anneal at 900, 1000, or 1200 °C for each specimen of (a). (c) The concentrations of N–O STDs formed by the 650 °C/8 h anneal for the NCZ silicon specimens with the pre-anneal at 900, 1000, or 1200 °C for 1–8 h. Herein, the abscissa represents the pre-annealing time.

precipitates that are further coarsened during the pre-anneal at 900, 1000, or 1200 °C. Consequently, the concentration of N–O STDs formed by the subsequent anneal at 650 °C is reduced due to the prolonged pre-anneal at 900, 1000, or 1200 °C.

So far, the reason for the result of Fig. 1 can be essentially understood as follows. With the 1000 °C/2 h pre-anneal during which the grown-in oxide precipitates are somewhat coarsened, (N_2)s are nearly annihilated in the meantime as shown in Fig. 2(b). Thus, the N–O STDs are hardly generated by the subsequent anneal at 650 °C. While, with the 1200 °C/2 h pre-anneal, only the grown-in oxide precipitates with considerably large sizes can grow up, during which the involved N impurities are limited. Thus, a considerable amount of (N_2)s survive, leading to the remarkable formation of N–O STDs in the subsequent anneal at 650 °C. In the case with the 900 °C/2 h pre-anneal, the amount of (N_2)s survived from the growth of grown-in oxide precipitates and, therefore, the concentration of N–O STDs lies in between the two cases with the 1000 °C/2 h and 1200 °C/2 h pre-anneals, respectively.

Figure 3(a) shows the 8 K far-infrared FTIR spectra for the NCZ silicon specimens annealed at 650 °C for 8 h, following the pre-anneals of 1000 °C/8 h and 1000 °C/8 h + 1250 °C/2 h, respectively. As can be known, the N–O STDs are hardly generated in the specimen with only the 1000 °C/8 h pre-anneal, while a considerable number of N–O STDs are formed in the specimen with the two-step pre-anneal of 1000 °C/8 h + 1250 °C/2 h. Figure 3(b) illustrates the middle-infrared FTIR spectra for the specimens subjected to the pre-anneals of 1000 °C/8 h and 1000 °C/8 h + 1250 °C/2 h, respectively. As seen, with the additional 1250 °C/2 h anneal, the (N_2)-related 963 cm^{-1} absorption peak significantly reappears. Definitely, Figs. 3(a) and 3(b) again evidence that the existence of (N_2)s is necessary for the generation of N–O STDs. After the 1000 °C/8 h pre-anneal, the growth of the grown-in oxide precipitates is considerably significant as indicated in Fig. 2(a), which is accompanied by the annihilation of (N_2)s, as revealed by no discernible 963 cm^{-1} absorption peak in Fig. 3(b). With the additional 1250 °C/2 h anneal, most of the oxide precipitates are dissolved, leading to the remarkable regeneration of (N_2)s, as revealed by the pronounced 963 cm^{-1} absorption peak in Fig. 3(b). Therefore, it has been unequivocal that the existence of (N_2)s is strongly dependent on the degree of OP in NCZ silicon.

Thus far, it can be believed that the loss of (N_2)s arisen from the pre-anneal at 900, 1000, or 1200 °C and the consequent effects on the formation of N–O STDs at 650 °C, as revealed in Figs. 1 and 2, are due to that the N impurities participate in the growth of grown-in oxide precipitates in a specific way. In the following, the capture of N impurities by the oxide precipitates, on the one hand, and the release of N impurities from the oxide precipitates, on the other hand, will be investigated in order to understand how the N impurities participate in the growth of grown-in oxide precipitates.

C. Capture of N impurities by the oxide precipitates

In order to understand the correlation between the loss of (N_2)s and growth of grown-in oxide precipitates, we have designed the following experiment from another point of view. The conventional CZ silicon specimens are first subjected to the specific anneals to form different amounts of oxide precipitates. Subsequently, they are subjected to the RTA terminated at 1250 °C in N_2 ambient for introducing N impurities. Finally, the concentrations of (N_2)s in such treated CZ silicon specimens are qualitatively compared by means of RT FTIR characterization. To this end, CZ-A, B, and C silicon specimens were prepared by the annealing

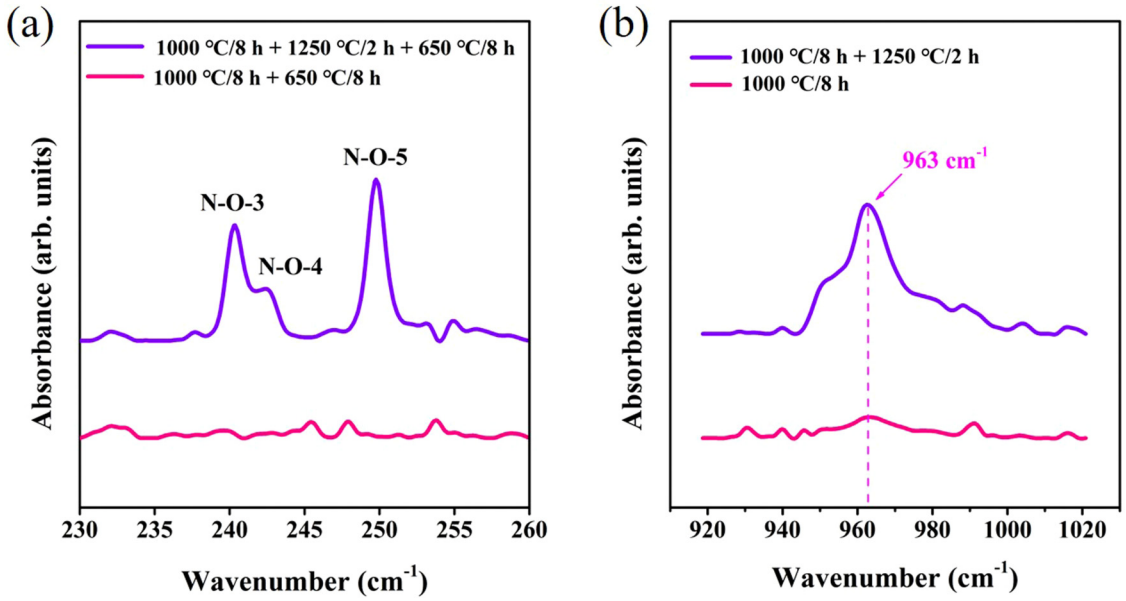

FIG. 3. (a) 8 K far-infrared FTIR spectra for the NCZ silicon specimens annealed at 650 °C for 8 h, following the pre-anneals of 1000 °C/8 h and 1000 °C/8 h + 1250 °C/2 h, respectively. (b) RT middle-infrared FTIR spectra for the NCZ silicon specimens subjected to pre-anneals of 1000 °C/8 h and 1000 °C/8 h + 1250 °C/2 h, respectively.

schemes as listed in Table II. Therein, CZ-A specimen hardly contains oxide precipitates, while CZ-B specimen contains oxide precipitates, which are much fewer than those in the CZ-C counterpart.

Figure 4(a) shows the depth profiles of N concentrations in CZ-A, B, C specimens within the depth of first 5 μm, measured by SIMS. As seen, the three depth profiles are nearly identical. Strictly, the concentration of the RTA-introduced N impurities in each specimen should decrease gradually from the surface to the bulk according to the law of diffusion. However, due to the extraordinarily fast diffusion of N in silicon,[43] the distribution of N impurities within the depth of first 5 μm is considerably uniform, as shown in Fig. 4(a). Anyhow, in can be deemed that the concentrations of N impurities in CZ-A, B, and C specimens introduced by the 1250 °C/60 s RTA in N_2 ambient are almost identical. The mechanism for the introduction of N impurities into silicon through the high temperature RTA in N_2 ambient will be discussed in other work.

Figure 4(b) shows the RT middle-infrared FTIR spectra of CZ-A, B, and C specimens. Herein, only the 963 cm^{-1} absorption peaks associated with (N_2)s are illustrated, because no absorption peaks of N-related complexes such as N–O complexes appear in the FTIR spectra. As seen, the 963 cm^{-1} absorption peak intensities of CZ-A, B, and C specimens decrease successively, indicating that the concentrations of (N_2)s in CZ-A, B, and C specimens decrease, in turn, although the total concentrations of N impurities in the three specimens are almost identical. As shown in Fig. 4(c), the amounts of oxide precipitates in CZ-A, B, and C specimens increase successively. Thus, from Figs. 4(b) and 4(c), it can be inferred that the more the oxide precipitates, the more significant the loss of (N_2)s is. Generally, the N impurities, which are not captured or combined by other entities in silicon, are almost in the form of (N_2)s at RT.[15] Therefore, it can be derived that a number of N impurities introduced by the 1250 °C/60 s RTA in N_2 ambient have been captured by the existing oxide precipitates in CZ-B or C specimen. Then, the uncaptured N impurities almost exist in the form of (N_2)s at RT. Evidently, more N impurities will be captured by the larger amount of oxide precipitates in CZ-C specimen, thus resulting in a more significant loss of (N_2)s. It should be stated that the capture of N impurities by the oxide precipitates is essentially arisen from the diffusion of N impurities toward the oxide precipitates. At elevated temperatures, the N impurities in silicon exist in both forms of (N_2)s and N_i atoms and the proportion of N_i atoms increases with the temperature.[15,17] Moreover, it has been documented that the diffusion of N impurities in silicon proceeds via the form of N_i atom.[43,45] Concretely, an N_i atom migrates from the three-bonded split interstitial site to a two-bonded bridge site and then back again, thereby completing the diffusion in the ⟨110⟩ orientation.[45] Therefore, it is derived that a part of N impurities introduced by the 1250 °C/60 s RTA in N_2 ambient diffuse in the form of N_i atoms toward the existing oxide precipitates in CZ-B or C specimen.

By the way, let CZ-A, B, and C specimens to be subjected to the 650 °C/8 h anneal for the formation of N–O STDs. Figure 4(d) shows the sequential decrease in the concentrations of N–O STDs in CZ-A, B, and C specimens with subsequent 650 °C/8 h anneal, again confirming the positive correlation between the concentration of N–O STDs and that of (N_2)s.

As for the location of the N impurities captured by the oxide precipitates, it can be qualitatively believed that the N_i atoms diffusing toward the oxide precipitates are most energetically favored to

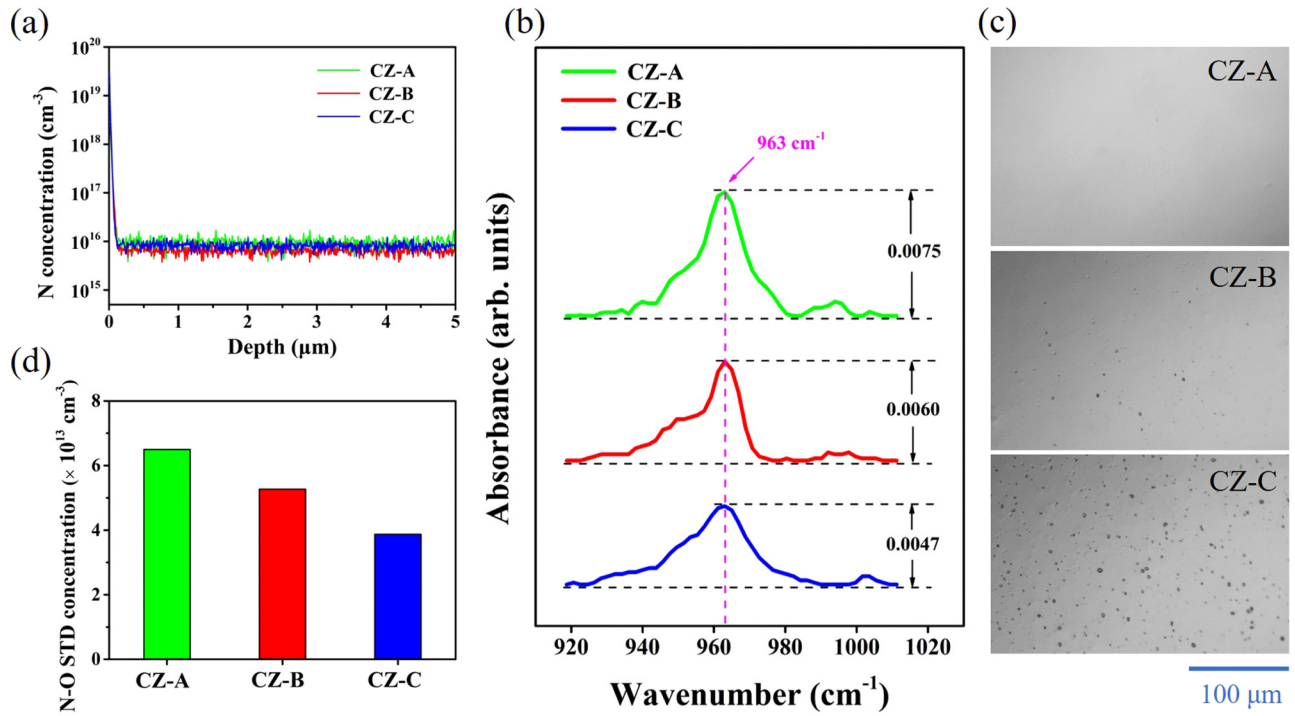

FIG. 4. (a) N concentration depth profiles, (b) RT FTIR spectra, and (c) OM images of BMDs for CZ-A, B, and C specimens. (d) Concentrations of N–O STDs generated in CZ-A, B, and C silicon specimens with subsequent 650 °C/8 h anneal. Note that the annealing schemes for CZ-A, B, and C silicon specimens are listed in Table II.

reside at the surfaces of oxide precipitates, more rigorously, at the interfaces between the oxide precipitates and silicon host (denoted as SiO_x/Si interfaces for simplicity, $1 < x < 2$). Intuitively, an energy barrier should be surmounted for the N_i atoms to diffuse into the oxide precipitates. Namely, the N impurities are not energetically favored to enter into the oxide precipitates. The aforementioned qualitative analysis will be supported by the following DFT calculations. As denoted above, the oxide precipitates are essentially of non-stoichiometric silicon oxide (SiO_x).[46–49] Kissinger and co-workers have derived that the values of x are between 1.7 and 2.[47] Therefore, there are always dangling bonds at the surfaces of oxide precipitates, which can be passivated by the N_i atoms diffusing from the NCZ silicon host. Moreover, the SiO_x/Si interfaces themselves facilitate the segregation of N impurities. For the two reasons above, the interfacial energies of oxide precipitates can be reduced by the incorporation of N impurities. In the aspect of experimental studies, Kvit *et al.* once investigated OP in NCZ silicon by transmission electron microscopy, finding that the N concentration at the oxide precipitate surface was much higher than those elsewhere.[50,51] Adam *et al.* reported that the N impurities implanted into the SiO_2 film on silicon substrates substantially aggregated at the SiO_2/Si interface after the anneals at 650–1050 °C.[52,53] In view of such previously reported results, it can be derived that the N impurities captured by the oxide precipitates are primarily located at the SiO_x/Si interfaces.

D. Release of N impurities from oxide precipitates

It has been learned from Fig. 3(b) that (N_2)s can be regenerated due to the substantial dissolution of the oxide precipitates in NCZ silicon. Nevertheless, it is not yet clear whether the regeneration of (N_2)s could occur if the oxide precipitates are insignificantly dissolved in NCZ silicon. Hence, the high temperature RTA is performed for the dissolution of oxide precipitates in NCZ silicon, herein, making it possible to investigate whether the regeneration of (N_2)s occurs as the oxide precipitates are little dissolved. Figures 5(a)–5(c) show the changes in the $[O_i]$, the 963 cm^{-1} IR absorption peak intensity and the BMDs related to the oxide precipitates, respectively, along with the time of RTA at 1250 °C for the NCZ silicon specimens with the 1000 °C/8 h pre-anneal, which has enabled the significant growth of grown-in oxide precipitates and the simultaneous annihilation of (N_2)s, as revealed in Figs. 2(a) and 2(b). On the abscissa of Fig. 5(a) or 5(b), the "null" represents no subsequent RTA and the "0" means no dwelling time at the RTA terminal temperature of 1250 °C. As can be seen, when the dwelling time at 1250 °C is less than 5 s, the increase in $[O_i]$ is slight, corresponding to nearly no discernible change in the BMD density, meaning that the oxide precipitates are little dissolved; while the 963 cm^{-1} absorption peak intensity increases significantly, indicative of the remarkable regeneration of (N_2)s. Particularly, it should be noted that, from "null" to "0," the increase

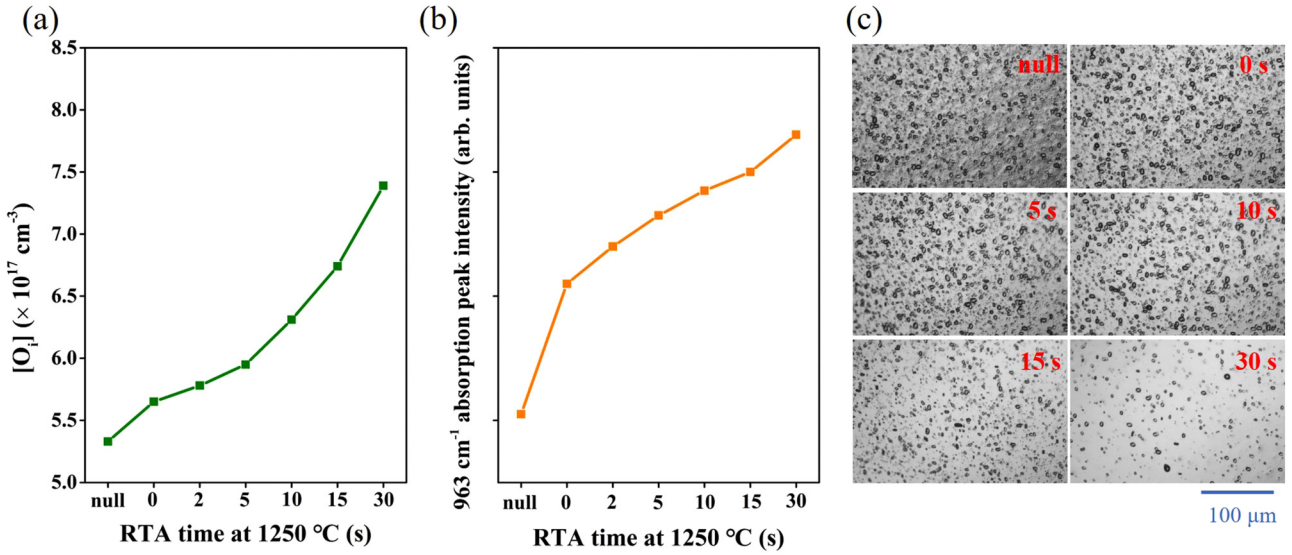

FIG. 5. The changes in (a) the $[O_i]$, (b) the 963 cm^{-1} absorption peak intensity, and (c) the BMDs related to the oxide precipitates, along with the time of RTA at 1250 °C for the NCZ silicon specimens with the 1000 °C/8 h pre-anneal. On the abscissa of (a) or (b) and at the upper-right corners of (c), the "null" represents no subsequent RTA and the "0" means no dwelling time at the RTA terminal temperature of 1250 °C. The RTA times are also shown at the upper-right corners of (c).

in the 963 cm^{-1} absorption peak intensity and, therefore, the regeneration of (N_2)s is the most significant [see Fig. 5(b)] even though the increase in $[O_i]$ is only 3.2×10^{16} cm^{-3} [see Fig. 5(a)] and the BMD density hardly changes [see Fig. 5(c)]. As the dwelling time at 1250 °C exceeds 5 s, $[O_i]$ increases more rapidly [see Fig. 5(a)], accompanied by the remarkable reduction of BMD density [see Fig. 5(c)], indicative of the significant dissolution of oxide precipitates. However, the increase in the 963 cm^{-1} absorption peak intensity becomes much slower [see Fig. 5(b)], indicating that the regeneration of (N_2)s is much weaker than that in the initial stage of RTA as mentioned above.

In brief, Fig. 5 reveals that the release of N impurities from the oxide precipitates and, therefore, the regeneration of (N_2)s do not necessitate the substantial dissolution of oxide precipitates in NCZ silicon. Furthermore, it can be deduced from Figs. 4 and 5 that during the growth of grown-in oxide precipitates in NCZ silicon

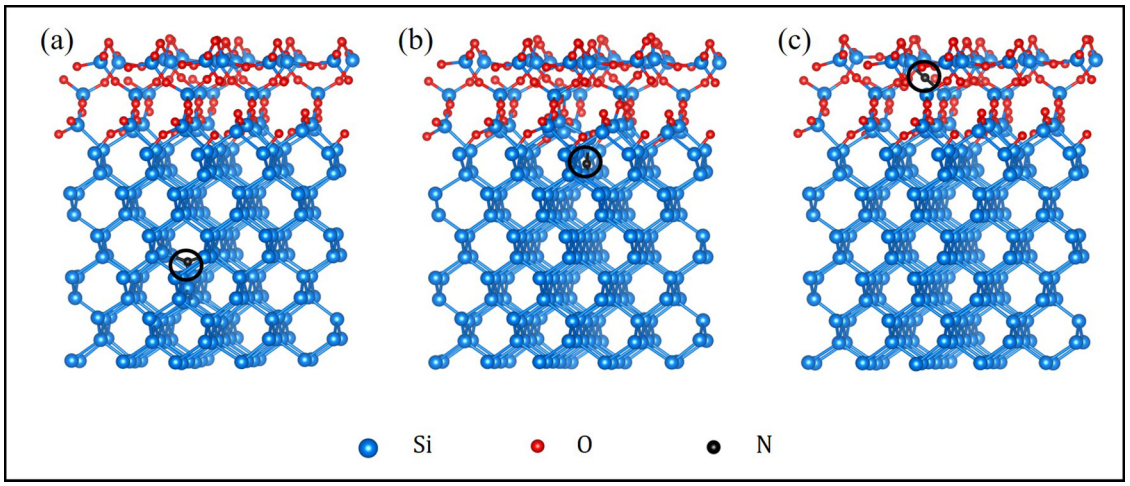

FIG. 6. The optimized structure of the supercell containing an N atom and an α-SiO_2/Si interface, where an N_i atom is located into the silicon host (a), an N atom passivates a Si dangling bond at the α-SiO_2/Si interface (b), and an N_i atom is located into the α-SiO_2 layer (c). Note that the N atom is circled by black in each supercell.

TABLE III. The energies of three optimized supercells in Fig. 6.

Supercell	(a)	(b)	(c)
Energy (eV)	−2256.15	−2256.78	−2252.03

subjected to the post-anneals at elevated temperatures, the N impurities, diffusing from the silicon host toward the oxide precipitates, are inclined to be captured at the SiO_x/Si interfaces, namely, at the surfaces of oxide precipitates. In this way, just the "thermal shock" at a high temperature (e.g., the RTA terminated at 1250 °C without a dwelling time) can enable the N impurities to be released from the oxide precipitates in NCZ silicon, which are substantially regenerated to be (N_2)s at low temperatures especially at RT.

E. DFT calculations

Figure 6 shows the optimized structure of the supercell containing an N atom and an α-SiO_2/Si interface, where an N_i atom is located into the silicon host (a), an N atom passivates a Si dangling bond at the α-SiO_2/Si interface (b), or an N_i atom is located into the α-SiO_2 layer (c). The energies of such three optimized supercells are listed in Table III. It can be seen that the energy of the supercell is lowest as the N atom is located at the α-SiO_2/Si interface, indicating that the SiO_2/Si interface is the energetically favorable site for the N atom to reside. Moreover, the energy of supercell is highest as the N atom is located into the α-SiO_2 layer, indicating that the diffusion of N atom into α-SiO_2 is not energetically favorable. It should be pointed out that the α-SiO_2 layer in the supercell used for the DFT calculations is of crystalline phase, while the oxide precipitates are generally of amorphous silicon oxide.[47,48] Nevertheless, the α-SiO_2 layer in each supercell herein contains only several atomic layers, and the amorphous silicon oxide is of short-range order within several atomic layers. Hence, it is reasonable to use α-SiO_2 to represent the oxide precipitate on the scale of the supercell used for the DFT calculations. In a word, the present results of DFT calculations reasonably support our experimentally derived viewpoint that the N impurities are inclined to reside at the SiO_x/Si interfaces during the growth of grown-in oxide precipitates in NCZ silicon. At the moment, it can be further deduced that the residing of N impurities at the SiO_x/Si interfaces is beneficial for reducing the Gibbs free energy for OP, thus facilitating the growth of grown-in oxide precipitates in NCZ silicon during the appropriate post-anneals.

V. CONCLUSIONS

The effects of pre-anneals at temperatures of 900–1200 °C for 2 h on the formation of N–O STDs in NCZ silicon at 650 °C have been first investigated. It is found that the formation of N–O STDs can be almost completely suppressed by the 1000 °C/2 h pre-anneal, while that is more significant after the 1200 °C/2 h pre-anneal than after the 900 °C/2 h one. Moreover, it is found that (N_2)s are nearly annihilated by the 1000 °C/2 h pre-anneal, while the concentration of remaining (N_2)s is much higher after the 1200 °C/2 h pre-anneal than after the 900 °C/2 h one. Furthermore, it is revealed that the concentration of (N_2)s is constantly decreased along with the growth of grown-in oxide precipitates during the pre-anneal at 900–1200 °C for 1–8 h. Correspondingly, the concentration of N–O STDs formed by the subsequent 650 °C anneal is also constantly decreased. The aforementioned experimental results indicate that the more significant growth of grown-in oxide precipitates during the pre-anneal, which consumes much more N impurities, leads to forming much fewer N–O STDs. This finding stimulates us to learn how the N impurities participate in the growth of grown-in oxide precipitates, which can enable us to essentially understand the pre-annealing effects on the formation of N–O STDs. On the one hand, the total N concentrations and the concentrations of (N_2)s have been investigated for the conventional CZ silicon specimens, which contain different amounts of oxide precipitates formed by the dedicated anneals, subjected to the 1250 °C/60 s RTA in N_2 ambient for the introduction of N impurities. It is found that, with the almost identical concentration of N impurities introduced by the aforementioned RTA, the concentration of (N_2)s decreases with the increase in oxide precipitates in the CZ silicon slices investigated. This fact indicates that a part of N impurities are captured by the existing oxide precipitates, leading to the decrease in the concentration of (N_2)s. It is believed that the captured N impurities are located at the SiO_x/Si interfaces, which is the most energetically favorable. On the other hand, the change in the concentration of (N_2)s along with the dissolution of oxide precipitates, which resulted from the RTA terminated at 1250 °C for different dwelling times, has been investigated for the NCZ silicon specimens subjected to the 1000 °C/8 h pre-anneal that has enabled the significant growth of grown-in oxide precipitates and the simultaneous annihilation of (N_2)s. It is found that (N_2)s can be significantly regenerated even if the oxide precipitates are little dissolved, reasonably indicating that most of the N impurities participating in the growth of grown-in oxide precipitates reside at the SiO_x/Si interfaces. The DFT calculation results hint that the N atoms are energetically favored to reside at the SiO_x/Si interfaces rather than to enter into the oxide precipitates. In a word, this work has clarified the correlation between the formation of N–O STDs and the growth of grown-in oxide precipitates, which tells us that the N impurities participating in the growth of grown-in oxide precipitates predominately reside at the SiO_x/Si interfaces.

ACKNOWLEDGMENTS

The authors acknowledge financial support from the Natural Science Foundation of China (NSFC) (Grant Nos. 62174145 and 61721005) and the Zhejiang Provincial Key R&D project (No. 2020C01009). The authors also thank Professor Yunhao Lu from the Department of Physics, Zhejiang University for help with DFT calculations.

AUTHOR DECLARATIONS

Conflict of Interest

The authors have no conflicts to disclose.

DATA AVAILABILITY

The data that support the findings of this study are available from the corresponding author upon reasonable request.

REFERENCES

[1]M. Suezawa, K. Sumino, H. Harada, and T. Abe, Jpn. J. Appl. Phys., Part 2 **25**, L859–L861 (1986).
[2]P. Wagner, R. Oeder, and W. Zulehner, Appl. Phys. A **46**, 73–76 (1988).
[3]M. Suezawa, K. Sumino, H. Harada, and T. Abe, Jpn. J. Appl. Phys., Part 1 **27**, 62–67 (1988).
[4]A. Hara, T. Fukuda, T. Miyabo, and I. Hirai, Appl. Phys. Lett. **54**, 626–628 (1989).
[5]J. A. Griffin, J. Hartung, J. Weber, H. Navarro, and L. Genzel, Appl. Phys. A **48**, 41–47 (1989).
[6]A. G. Steele, L. C. Lenchyshyn, and M. L. W. Thewalt, Appl. Phys. Lett. **56**, 148–150 (1990).
[7]C. Hu, Y. Huang, H. Ye, S. Shen, and M. Qi, Appl. Phys. Lett. **59**, 2260–2262 (1991).
[8]C. Chen, C. Li, H. Ye, S. Shen, and D. Yang, J. Appl. Phys. **76**, 3347–3350 (1994).
[9]R. Jones, C. Ewels, J. Goss, J. Miro, P. Deak, S. Oberg, and F. B. Rasmussen, Semicond. Sci. Technol. **9**, 2145–2148 (1994).
[10]D. Yang, R. Fan, L. Li, D. Que, and K. Sumino, Appl. Phys. Lett. **68**, 487–489 (1996).
[11]R. C. Newman, J. H. Tucker, N. G. Semaltianos, E. C. Lightowlers, T. Gregorkiewicz, I. S. Zevenbergen, and C. A. J. Ammerlaan, Phys. Rev. B **54**, R6803–R6806 (1996).
[12]X. Shi, P. Liu, and S. Shen, Appl. Phys. Lett. **69**, 3549–3550 (1996).
[13]H. C. Alt and H. E. Wagner, Phys. Rev. B **82**, 115203 (2010).
[14]V. V. Voronkov, M. Porrini, P. Collareta, M. G. Pretto, R. Scala, R. Falster, G. I. Voronkova, A. V. Batunina, V. N. Golovina, L. V. Arapkina, A. S. Guliaeva, and M. G. Milvidski, J. Appl. Phys. **89**, 4289–4293 (2001).
[15]R. Jones, S. Öberg, F. Berg Rasmussen, and B. Bech Nielsen, Phys. Rev. Lett. **72**, 1882–1885 (1994).
[16]F. B. Rasmussen and B. B. Nielsen, Phys. Rev. B **49**, 16353–16360 (1994).
[17]H. Sawada and K. Kawakami, Phys. Rev. B **62**, 1851–1858 (2000).
[18]C. P. Ewels, R. Jones, S. Öberg, J. Miro, and P. Deák, Phys. Rev. Lett. **77**, 865–868 (1996).
[19]H. C. Alt, H. E. Wagner, W. v. Ammon, F. Bittersberger, A. Huber, and L. Koester, Physica B **401–402**, 130–133 (2007).
[20]H. E. Wagner, H. C. Alt, W. von Ammon, F. Bittersberger, A. Huber, and L. Koester, Appl. Phys. Lett. **91**, 152102 (2007).
[21]H. C. Alt and H. E. Wagner, J. Appl. Phys. **106**, 103511 (2009).
[22]T. Zhao, C. Hua, W. Lan, Y. Sun, D. Wu, Y. Lu, X. Ma, and D. Yang, J. Appl. Phys. **129**, 145702 (2021).
[23]T. Y. Tan, E. E. Gardner, and W. K. Tice, Appl. Phys. Lett. **30**, 175–176 (1977).
[24]D. Gilles, E. R. Weber, and S. Hahn, Phys. Rev. Lett. **64**, 196–199 (1990).
[25]R. J. Falster, G. R. Fisher, and G. Ferrero, Appl. Phys. Lett. **59**, 809–810 (1991).
[26]H. Hieslmair, A. A. Istratov, S. A. McHugo, C. Flink, T. Heiser, and E. R. Weber, Appl. Phys. Lett. **72**, 1460–1462 (1998).
[27]F. Shimura and R. S. Hockett, Appl. Phys. Lett. **48**, 224–226 (1986).
[28]K. Aihara, H. Takeno, Y. Hayamizu, M. Tamatsuka, and T. Masui, J. Appl. Phys. **88**, 3705 (2000).
[29]K. Nakai, Y. Inoue, H. Yokota, A. Ikari, J. Takahashi, A. Tachikawa, K. Kitahara, Y. Ohta, and W. Ohashi, J. Appl. Phys. **89**, 4301–4309 (2001).
[30]X. Yu, D. Yang, X. Ma, J. Yang, L. Li, and D. Que, J. Appl. Phys. **92**, 188–194 (2002).
[31]X. Yu, D. Yang, X. Ma, and D. Que, Microelectron. Eng. **69**, 97–104 (2003).
[32]G. Kissinger, T. Müller, A. Sattler, W. Häckl, M. Weber, U. Lambert, A. Huber, P. Krottenthaler, H. Richter, and W. von Ammon, Solid State Phenom. **108–109**, 17–24 (2005).
[33]C. Cui, D. Yang, X. Ma, and D. Que, Jpn. J. Appl. Phys. **45**, 4903–4907 (2006).
[34]G. Kissinger, U. Lambert, M. Weber, F. Bittersberger, T. Müller, H. Richter, and W. von Ammon, Phys. Status Solid A **203**, 677–684 (2006).
[35]G. Kresse and J. Furthmüller, Comput. Mater. Sci. **6**, 15–50 (1996).
[36]G. Kresse and J. Furthmüller, Phys. Rev. B **54**, 11169–11186 (1996).
[37]J. Hafner, J. Comput. Chem. **29**, 2044–2078 (2008).
[38]J. P. Perdew, K. Burke, and M. Ernzerhof, Phys. Rev. Lett. **77**, 3865–3868 (1996).
[39]J. P. Perdew, K. Burke, and Y. Wang, Phys. Rev. B **54**, 16533–16539 (1996).
[40]B. Delley, J. Chem. Phys. **113**, 7756–7764 (2000).
[41]A. Kanamori and M. Kanamori, J. Appl. Phys. **50**, 8095–8101 (1979).
[42]H. C. Alt and H. E. Wagner, Physica B **407**, 2985–2988 (2012).
[43]V. V. Voronkov and R. J. Falster, Solid State Phenom. **95–96**, 83–92 (2003).
[44]A. Borghesi, B. Pivac, A. Sassella, and A. Stella, J. Appl. Phys. **77**, 4169–4244 (1995).
[45]P. A. Schultz and J. S. Nelson, Appl. Phys. Lett. **78**, 736–738 (2001).
[46]A. Borghesi, A. Piaggi, A. Sassella, A. Stella, and B. Pivac, Phys. Rev. B **46**, 4123–4127 (1992).
[47]D. Kot, G. Kissinger, M. A. Schubert, M. Klingsporn, A. Huber, and A. Sattler, Phys. Status Solidi RRL **9**, 405–409 (2015).
[48]G. Kissinger, M. A. Schubert, D. Kot, and T. Grabolla, ECS J. Solid State Sci. Technol. **6**, N54–N63 (2017).
[49]G. Kissinger, D. Kot, A. Huber, R. Kretschmer, T. Müller, and A. Sattler, ECS J. Solid State Sci. Technol. **9**, 064002 (2020).
[50]G. A. Rozgonyi, A. Karoui, A. Kvit, and G. Duscher, Microelectron. Eng. **66**, 305–313 (2003).
[51]A. Kvit, A. Karoui, G. Duscher, and G. A. Rozgonyi, Appl. Phys. Lett. **84**, 1889–1891 (2004).
[52]L. S. Adam, M. E. Law, K. S. Jones, O. Dokumaci, C. S. Murthy, and S. Hegde, J. Appl. Phys. **87**, 2282–2284 (2000).
[53]L. S. Adam, M. E. Law, O. Dokumaci, Y. Haddara, C. Murthy, H. Park, S. Hegde, D. Chidambarrao, S. Mollis, T. Domenicucci, C. Dziobkowski, K. Jones, P. Wong, R. Young, and R. Srinivasan, Mater. Res. Soc. Symp. Proc. **568**, 277–281 (1999).